Quantification of Edematic Effects in Prostate Brachytherapy Interventions

Mohamed Hefny, Purang Abolmaesumi, Zahra Karimaghaloo, David G. Gobbi, Randy Ellis, and Gabor Fichtinger

School of Computing, Queen's University, Kingston, Ontario, Canada
gabor@cs.queensu.ca

Abstract. We present a quantitative model to analyze the detrimental effects of edema on the quality of prostate brachytherapy implants. We account for both tissue expansion and implant migration by mapping intra-operative ultrasound and post-implant CT. We pre-process the ultrasound with a phase congruency filter, and map it to the volume CT using a B-spline deformable mutual information similarity metric. To test the method, we implanted a standard training phantom with 48 seeds, imaged the phantom with ultrasound and CT and registered the two for ground truth. Edema was simulated by distorting the CT volume by known transformations. The objective was to match the distorted implant to the intra-operative ultrasound. Performance was measured relative to ground truth. We successfully mapped 100% of deformed seeds to ground truth under edematic expansion up to 40% of volume growth. Seed matching performance was 98% with random seed migration of 3mm superimposed on 10% edematic volume growth. This method promises to be clinically applicable as the first quantitative analysis tool to measure edematic implant deformations occurring between the operating room and post-operative CT imaging.

1 Introduction

With 225,000 new cases and 33,000 deaths annually, prostate cancer remains the most common cancer and the second leading cause of death in American men [1]. Low-dose-rate permanent brachytherapy (brachytherapy hereafter) has emerged as one of the definitive treatment modalities for prostate cancer. The procedure entails permanent transperineal implantation of 50 to 150 small radioactive pellets (aka seeds) into the prostate under real-time transrectal ultrasound (TRUS) guidance [2]. Annually, over 50,000 such procedures are performed in North America [3], and the demand has been rising steadily, though it has temporarily decelerated due to the recent media campaign for robotic prostate resection. A critical element in brachytherapy is correct seed placement, since faulty seed placement can cause insufficient dose to the cancer and/or inadvertent radiation of the rectum, urethra and bladder. The former causes failure of treatment, while the latter results in adverse side-effects like rectal ulceration, dysuria (painful urination) and incontinence. Despite strict control of the intra-operative workflow, edema may occur and cause significant dosimetric uncertainties; an issue under intense clinical investigation. Next to faulty source placement, edema is the most significant cause of failure in localized prostate therapies [4]. If edematic

D. Metaxas et al. (Eds.): MICCAI 2008, Part II, LNCS 5242, pp. 493–500, 2008.

fluid accumulates in the prostate, cancerous tissues receive proportionally less dosage and the cancer may eventually recur [5]. Edema may onset immediately after needle placement begins and continues to evolve during the procedure [2]. In a recent study, Tanaka *et al*. found that edema caused 30% average increase in prostate volume on the first day after implantation [6]. Edema typically subsides after 2-4 weeks with a half-life of 10 days [7]; however, by then much of the dose is already delivered due to the short half-life of the isotopes (Pd103=17 days, I125=60 days). The degree of edema varies from patient to patient with no apparent predictive factors for its magnitude or detrimental effects on implant dosimetry. Striking as it sounds, in contemporary practice patients are released from the operating room without analysis or quantitative measurement of seed positions and dosimetry, and the implant dosimetry is not evaluated until the post-operative CT.

Interestingly, edema is considered as a major factor in the optimal timing of the post-implant CT [8]. Prior works only looked at edematic volume growth by contouring the prostate gland, but we are still not able to tell whether an implant failed because of inadequate implantation, or because a perfectly executed implant was distorted by the ensuing edema. Currently there is no quantitative understanding of how the implant (i.e. location of implanted seeds) and the resulting dosimetry change between being completed in the operation and before it is first evaluation in post-operative CT. In absence of such quantitative data, we cannot even start guessing the statistical nature of changes or any positive correlation between edema and the choice of seed locations relative to the internal prostate anatomy. In order to be able to approach these fundamental clinical questions, we must map the intra-operative TRUS with post-operative CT and discern the dislocation of seeds and relevant anatomy. Seeds are well-tractable in CT due to their high contrast to the soft tissue background, but mapping post-implant CT to intra-operative TRUS is rather challenging. Large edematic tissue expansion, apparent seed migration, perturbations, anatomical deformation caused by changes in body position from lithotomy to supine, and changes of rectal pressure make registration difficult to achieve. In this paper we present the design, implementation and analysis, of a method that can cope with these problems. We track the motion of actual seeds, while prostate contouring remains still available to characterize the shape and size of the organ.

2 Methods

TRUS is generally adequate for visualizing the prostate, but it suffers from many artifacts such as speckle, air-cavities, acoustic shadowing, reverberations, and multiple reflections. Because of this, in a fully implanted prostate, TRUS does not allow for robust and accurate localization of the implanted seeds. There have been recent efforts to register TRUS with intra-operative fluoroscopy for the purpose of in-room dosimetry, in which case there is no deformation and seed motion. In these studies, seeds were segmented from both TRUS and fluoroscopy and registered with a variant of ICP [9] and network flow-based methods [10]. These segmentation-based methods are not sufficiently accurate and robust in a rigid and motionless case, so they cannot be expected to work in our case with large tissue expansions and seed migration. Hence, we thought of intensity-based registrations, following a procedure as shown in

Figure 1. We pre-process the images with filters, compound the TRUS and CT volumes, and then apply B-spline deformable mutual information (MI) based registration. The basic objective in pre-filtering the volumes is to enhance seed-like regions without explicit segmentation of them. As seed-like regions are usually prominent in CT imaging, MI can lock on to these mutually pronounced regions.

Filtering: We set the region of interest around the prostate gland and apply simple window-level linear mapping in the CT volume. In the TRUS volume too, we set a region of interest around the gland and linearly scale the intensities to the same range as the CT volume, to facilitate subsequent MI registration. Previously, Hacihaliloglu *et al.* used the phase congruency (PCON) approach for detecting bone edges in ultrasound images [11]. Here, we use PCON to enhance features of true seeds by suppressing artifacts and false positives. PCON evaluates features based on phase rather than amplitude information. Since it gives a measure of significance for each point invariantly to image brightness or contrast, a constant and uniform threshold can be applied to extract feature points from the phase information [12]. We calculate the PCON at each pixel of each image in order to measure the phase symmetry. The more symmetrical the phase of a region is, the more likely it is to be a seed. The measure of symmetry is calculated as the weighted average resulting from even and odd symmetry filters; because at symmetry points, the absolute values resulting from even and odd symmetry filters are large and small, respectively.

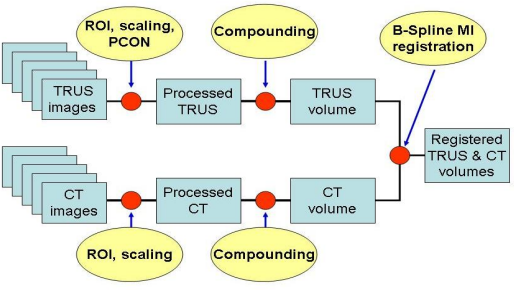

Fig. 1. Processing pipeline for TRUS-CT registration

Registration: We use B-spline deformable transformation with Mattes MI 3D metric. Edematic expansion offers itself to spline registration, where transformations interpolate control points extracted from both the source and target images to calculate the displacement required. Control points are selected using the MI similarity-based measure. B-spline is perhaps the most commonly used variant for spline interpolation in medical image registration, so it was a logical choice to try.

Ground Truth Phantom: Figure 2 on the next page shows an experimental ground truth phantom setup. The figure shows the relevant coordinate frames and transformations. We do not explain these in full details here, since the process and notations are assumed to be familiar from basic surgical navigation literature. We made a realistic implant in a phantom (CIRS, Norfolk, VA) with 48 seeds, arranged a set of 1mm CT fiducials on the container box, and acquired a CT volume with 0.3mm pixel size and 0.62mm slice thickness. We carefully segmented the seeds from the CT and converted their locations to the coordinate frame defined by the fiducials, which we localized with a calibrated pointer (Traxtal Inc., Toronto, ON) and Certus optical tracker (NDI,

Waterloo, ON). We calibrated the TRUS probe [13], collected a series of tracked US images from the phantom, and compounded the images to form a 3D volume. Finally, when the CT and TRUS volumes were registered, the seeds that we had segmented earlier from CT became known in the TRUS volume, providing us with accurate experimental ground truth. The fiducials and tracking bodies were arranged so that their centroids fell close to the center of the prostate to maximize our tracking accuracy.

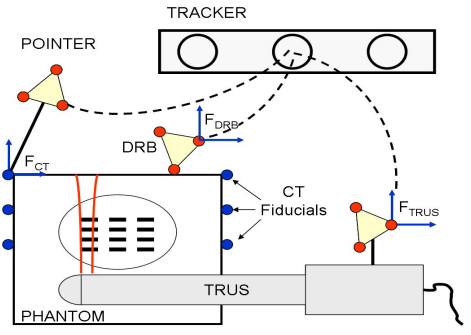

Fig. 2. Coordinate transformations in Ground Truth Phantom. Calibrated pointer is used to register the CT to the dynamic reference body (DRB). The TRUS probe is tracked relative to the DRB. Edematic expansion and seed migration were added computationally to the CT.

Edema Simulation: So far, the ground truth phantom data does not involve edematic expansion and seed motions. In lieu of expanding edema phantoms, we produced these effects purely computationally. Based on clinical literature, we estimate the edematic swelling with isotropic volume expansion [14]. This model is a fair one, since edema is caused by the physical trauma of the needle and seed insertions, and these are roughly uniformly distributed in the prostate volume. In actual implants, seed migrations and perturbations are superimposed on edematic swelling. Each seed travels with the swelling tissue and demonstrates its own motion and perturbation, seemingly independently from other seeds or the prostate itself. We model this effect with adding random noise of variable amplitudes to the location and orientation of the seeds. The CT volume was therefore transformed as follows. Seeds had been segmented earlier and their centroids were known. For each seed, a small container box around the centroid was determined to fully include the seed. The seed boxes were digitally removed from the volume and the remaining intensities were smoothed with tri-linear interpolation. The seedless volume was expanded to simulate the edematic swelling. For each seed, the volume expansion transformation was applied to the centroid of the seed box. The seed boxes were not expanded, since the seeds themselves do not expand. To simulate seed motion and perturbation, translation and orientation noise was applied to each seed box via a transformation with tri-linear interpolation before the box was inserted back into the swollen volume. The amplitude of the swelling, and the location and direction noise were the variable parameters of the simulation. It is important to emphasize the edema model was applied in creating the ground truth test data and it has no bearing on the registration performance in actual human implant cases. Isotropic swelling, random migration and random perturbation might be refined later, after we have found out more about the statistical nature of the edema process. Here, we are making the first quantitative analysis tool to characterize this process, and present clinical literature does not suggest better or even alternative models.

3 Results and Discussion

To verify the reliability of our quantification methodology, we performed different edema simulations using: capture range, prostate volumetric expansion, individual seeds migrations, and perturbation. We generated five different datasets with volumetric expansion from 0% to 45% percent, with 5% steps of the total prostate volume. For each dataset, we applied a random translation, with uniform distribution function, to each seed center of mass in the '*z*' direction, i.e. approximate direction of the needle insertion paths. It is because random seed migration is not quite symmetrical in actual implants. Migration along the needle tends to dominate and dislocations orthogonally to the needle path seem almost negligible. We varied the seed migration range between ±1mm and ±5mm, with 1mm steps. We also applied random seed rotations between ±5 degrees and ±20 degrees. We applied volume transformations between the ranges ±5mm translations and ±10 degrees rotations.

In actual brachytherapy procedures, initial pose estimation between TRUS and CT is very accurate and robust. The workflow is strictly controlled [2], allowing for precise determination of the directions of the main symmetry axes of the prostate. For CT imaging, we position the patient in supine pose with an empty rectum. For TRUS imaging, we place the patient in lithotomy position with the TRUS probe in the rectum. Here, we refer to external beam radiotherapy where the patient is repositioned in supine pose and we never compensate for rotational positioning errors of the prostate. This fact assures that with careful patient setup we can control prostate rotations about the lateral and AP axes very accurately, well within the capture range of our registration. The pitch angle of the prostate is also well-controlled by the setup, because for TRUS imaging the legs are held in stirrups of standard separation and elevation. The pitch angle of the prostate can be conveniently determined by fitting a standard ellipsoidal model on the midsection of the prostate capsule contoured in both TRUS and CT [15]. For all practical purposes, it is also safe to assume that false positives and missing seed appearances are approximately uniformly distributed in the CT and TRUS volumes. What follows is that after simple binary thresholding of the two volumes, the two gravity centers are practically identical. Jain *et al.* found this approach to be accurate to a few millimeters in intra-operative registration of C-arm fluoroscopy and TRUS of brachytherapy implants [16]. All said, we are confident that in actual clinical cases the initial pose will be conveniently determined within the capture range.

We used ITK B-spline deformable transformation with Mattes MI 3D metric, to register the pre-processed TRUS and transformed CT volumes. We measured the Euclidean distance between each seed registration and the ground truth. Since our method is essentially a correspondence algorithm, the percentage of correctly matched seeds, with mean error and SD is the most informative metrics to evaluate registration performance. The practical requirement for brachytherapy seed localization is about 2.0mm (the diameter of the implant needle), which we consider as the threshold for successful registration and matching between seeds.

According to Table 1, our registration pipeline produced 100% matching and correct registration for up 40% volumetric isotropic expansion. The matching rate drops just slightly, to 98%, when a really severe 45% expansion is applied. All the while, the mean registration error remains under 0.35mm, which must be considered as an outstanding result from clinical perspective.

Table 1. Volumetric expansion

Volumetric Expansion (%)	Mean Registration Error in (mm)	SD (mm)	Successful Registrations
10%	0.08	0.05	100%
20%	0.30	0.08	100%
30%	0.19	0.12	100%
40%	0.22	0.33	100%
45%	0.35	0.82	98%

Table 2. Seeds perturbation with 10% volumetric expansion

Seed Perturbation (degree)	Mean Registration Error in (mm)	SD (mm)	Successful Registrations
[-5,+5]	1.30	0.59	98%
[-10,+10]	1.53	0.24	98%
[-15,+15]	1.02	0.38	92%
[-20,+20]	1.34	0.49	92%

Table 2 shows registration performance with uniform random seeds orientation perturbation at a volume expansion of 10%. The average registration error remains well below the clinical threshold, while we receive a 98% matching rate at ±10 degrees random rotation and 92% matching rate at ±20 degrees random rotation.

Table 3. Seed migration with 10% volumetric expansion

Seed Migration (mm)	Mean Registration Error in (mm)	SD (mm)	Successful Registrations
[-1,+1]	1.20	0.39	100%
[-2,+2]	1.23	0.40	98%
[-3,+3]	1.42	0.39	95%
[-4,+4]	1.38	0.43	95%
[-5,+5]	1.60	0.38	90%

Table 3 shows registration performance with uniform random seeds migration at a volume expansion of 10%. The average registration error holds up well below the clinical threshold, while we observe 95% matching rate at ±3mm random migration and 90% matching rate at ±5mm random migration.

To test capture range, we ran registrations at a very sever 45% volume expansion and ±5mm random migration, with random translation and angular misalignments of ±5mm and ±10 degrees, respectively. With the initial misalignment, the method achieved 95% successful registrations with volume expansion and 90% with random seeds migrations while the mean error and SD were within acceptable range.

Generally, the choice of adaptive thresholding and phase congruency (PCON) filtering of the ultrasound data seems justified by consistently satisfactory registration results. A full analysis of the use of PCON in MI-based registration has been carried out in [17] that investigates the registration of intra-operative TRUS and fluoroscopy. In their case, TRUS and fluoroscopy imaging are performed concurrently, where there

is only negligible deformation and seeds are practically motionless. Our baseline results (no edema, no seed migration) are in perfect agreement with those studies. Figure 3 shows the overly of TRUS and CT images before and after registration.

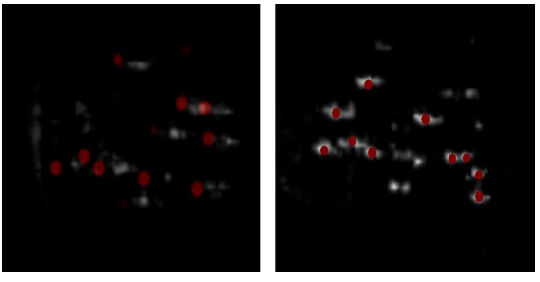

Fig. 3. Overly of TRUS and CT images on the same plane before (left) and after (right) registration

As to the choice of the B-spline deformable registration (BSDR), we had two motifs: its apparent suitability for coping with tissue swelling and its availability in the ITK open-source toolkit. A perennial problem of registration research is that one never knows the true reason of failure, whether the chosen registration method was inadequate or the coded implementation failed. As ITK offers the most stable and fully tested implementations, trying its BSDR seemed a logical choice. As the results show, BSDR was indeed eminently applicable to cope with isotropic tissue swelling, to very large degrees of volume growth, safely covering the extent of edematic swelling typically observed in actual implants [6]. BSDR is able to catch up with seed perturbation, though this is a clinically less important issue, because the dose field of an individual seed is relatively isotropic and symmetrical around the centroid [18]. More important is to handle translational migration, which BSDR did with somewhat less distinction. This was not completely un-anticipated, as B-spline is not very effective in following sharp curvatures that some seed constellations may cause in the deformation field. For example, if the random simulation casts two neighboring seeds to plus and minus 5mm, BSDR is not expected to be able to warp the field enough to capture such extremes. Luckily, however, "renegade seeds" often reveal themselves to the trained eye, so we can remove them from the CT before registration. It must be underscored that the primary endpoint of our edema characterization study is not dosimetry. The main objective is to understand statistical correlations between needle paths and edematic swelling and between implanted seed locations and seed migrations. Hence mismatched seeds are simply omitted from the statistics. In other words, as long as the registration error of correctly matched seeds remains low and the matching percentage remains reasonably high, we do not have to be concerned about "renegade seeds". These are seeds that migrate severely, sometimes up to over 10mm or more, in the ducts, needle tracts and blood vessels. With this in mind, BSDR performs quite well for us, yet there is still room and need for improvement.

Edema characterization is a post-operative process where speed does not signify. Pre-filtering the full TRUS volume took 13.0 sec in MATLAB. The ITK/C++ implementation of the B-spline deformable MI-based registration ran approximately 201.0 sec. We used an Intel Duo processor, with 1.66 GHz CPU and 2.00 GB RAM. Our software was not optimized for speed or memory efficiency.

In conclusion, the ability of quantitative measurement of edematic implant distortions may have significant impact on prostate brachytherapy. Our immediate objective will be to learn the true statistical nature of edema and its effect on implants. In the

extreme, we may conclude that pinpoint accuracy in the operating room is less critical, if post-implant edema tends to dominate the irradiation. This indeed would be a startling outcome with major consequences on clinical practice. (This work has been supported by U.S. NIH 1R01-CA111288 and Acoustic MedSystems, Inc.)

References

1. Jemal, A., et al.: Cancer statistics. CA Cancer J. Clin. 57(1), 43–66 (2007)
2. Wallner, K., et al.: Prostate brachytherapy made complicated, 2nd edn. SmartMedicine Press, Seattle (WA) (2001)
3. Cooperberg, M.R., et al.: The changing face of low-risk prostate cancer: trends in clinical presentation and primary management. J. Clin. Oncol. 1;22(11), 2141–2149 (2004)
4. Yamada, Y., et al.: Impact of intraoperative edema during transperineal permanent prostate brachytherapy on computer-optimized and preimplant planning techniques. Am. J. Clin. Oncol. 26(5), e130–135 (2003)
5. Roberson, P.L., et al.: Source placement error for permanent implant of the prostate. Med. Phys. 24, 251–257 (1997)
6. Tanaka, O., et al.: Effect of edema on postimplant dosimetry in prostate brachytherapy using CT/MRI fusion. Int. J. Radiat. Oncol. Biol. Phys. 69, 614–618 (2007)
7. Waterman, F.M., et al.: Edema associated with I-125 or Pd-103 prostate brachytherapy and its impact on post-implant dosimetry: An analysis based on serial CT acquisition. Int. J. Radiat. Oncol. Biol. Phys. 41, 1069–1077 (1998)
8. Prestidge, A.R., et al.: Timing of computed tomography-based postimplant assessment following permanent transperineal prostate brachytherapy. Int. J. Radiat. Oncol. Biol. Phys. 40, 1111–1115 (1998)
9. Su, Y., et al.: Seed localization and TRUS-fluoroscopy fusion for intraoperative prostate brachytherapy dosimetry. Computer Aided Surgery 12(1), 25–34 (2007)
10. Tutar, I.B., et al.: Seed-based ultrasound and fluoroscopy registartion using iterative optimal assignment for intraoperative prostate brachytherapy dosimetry. In: SPIE Medical Imaging, pp. 65091–650914 (2004)
11. Hacihalilogu, I., et al.: Enhancement of bone surface visualization from 3D ultrasound based on local phase information. In: IEEE Ultrasonics Symp., pp. 21–24 (2006)
12. Kovesi, P.: Image feature from phase congruency. In: Vider: A. J. of Comp. Vision Research, vol. 1(3), pp. 1–27. MIT press, Cambridge (1999)
13. Mercier, L., et al.: A review of calibration techniques for freehand 3-D ultrasound systems. Ultrasound Med. Biol. 31(4), 449–471 (2005)
14. Kim, Y., et al.: Dosimetric Impact of Prostate Volume Change Between CT-Based HDR Brachytherapy Fractions. Int. J. Radiat. Oncol. Biol. Phys. 59(4), 1208–1216 (2004)
15. Amink, R., et al.: Planimetric volumetry of the prostate: how accurate is it? Physiol. Meas. 16, 141–150 (1995)
16. Jain, A.K., et al.: Intra-operative Guidance in Prostate Brachytherapy Using an Average C-arm. In: Ayache, N., et al. (eds.) MICCAI 2007, Part II. LNCS, vol. 4792, pp. 9–16. Springer, Heidelberg (2007)
17. Karimaghaloo, Z., et al.: Intensity-Based Registration of Prostate Brachytherapy Implants and Ultrasound. In: 5th IEEE Int. Symp. on Biomed. Imag., pp. 780–783 (2008)
18. Yue, N., et al.: The impact of edema on planning 125I and 103Pd prostate implants. Med. Phys. 26, 763–767 (1999)